



UNIVERSAL WISER
PUBLISHER

Novel CaMoO₄@GO Nanocomposite: Synthesis, Characterization, and Investigation its Photocatalytic Properties

Seyed Mostafa Hosseinpour Mashkani

Young Researchers and Elites Club, Arak Branch, Islamic Azad University, Arak, Iran

E-mail: Hosseinpour.sm@gmail.com

Abstract: The current study aims to synthesize and characterize Calcium Molybdate-Graphene Oxide (CaMoO₄@GO) nanocomposite under ultrasonic irradiation. Primarily, degradation of Methylene blue (MB) under Uv-Vis light was investigated to measure the photocatalytic properties of the as-synthesized CaMoO₄@GO nanocomposite. In addition, various graphene oxide concentrations were applied to investigate its impact on the optical and photodegradation properties of calcium molybdate. X-ray diffraction (XRD), scanning electron microscopy (SEM), and spectra energy dispersive analysis of X-ray (EDS) were used to characterize CaMoO₄@GO nanocomposite. DRS results demonstrated that GO influenced significantly the optical properties of CaMoO₄ as much as band gap of CaMoO₄@GO nanocomposite shows a redshift in comparison with pure CaMoO₄. Consequently, photocatalytic results demonstrated that adding GO causes to increase photodegradation of MB from 65% (CaMoO₄) to 89% (CaMoO₄@GO).

Keywords: CaMoO₄@GO nanocomposite, ultrasonic method, photocatalytic, redshift

1. Introduction

In the third millennium, the human lifestyle has undergone huge changes due to the industrial revolution. As a result, various kinds of pollution including water, air, soil, noise, etc. have been emerging. Water pollution, as one of the main pollutions, damaged human life and the environment. Inorganic and organic dyes known as the main source of water pollution have been extensively used in different industries such as paper, plastics, textiles, and rubber industries. Over their advantages, they have many disadvantages including high toxicity, high environmental stability, and potentially irresolvable. There are many traditional techniques for treating dyes in wastewaters which are ineffective and costly^[1]. With introducing nanotechnology into the wastewater purification technologies, novel photocatalytic semiconductor nanomaterials have been developed. In the past decade, there has been a considerable attention to the semiconductor nanoparticles because of their unique physical properties which make them suitable for different applications^[2-9]. Besides, their ideal band gap makes them appropriate photocatalytic candidates for degradation of environmental pollutants such as detergents, pesticides, dyes, and volatile organic compounds under UV/Vis light^[10-16]. CaMoO₄ in which Ca atom exhibits eight-fold oxygen coordination and the Mo atom forms a MoO₄²⁻ tetrahedron, has gained lots of attention due to its high chemical stability. In addition, it's interesting luminescence properties which result of energy transfer from host lattice to the dopant ions (AMoO₄ (A = Ca, Sr, Ba))^[17-18] leading to its wide application in white light-emitting diodes, displays, and devices in photochemical fields^[19-22]. On the other hand, CaMoO₄ has potential applications in various areas including phosphor microparticles and acousto-optic filters, catalyst, microwave applications, solid-state lasers, phosphor microparticles, energy storage, the blue phosphor in fluorescent lighting devices and MASER materials, in medical applications as scintillator, humidity sensors, Li-ion batteries, fluorescent lamps, photoluminescence, photocatalytic, nano-pigment, etc^[23-26]. Various techniques have been used for synthesizing CaMoO₄ such as the Czochralski method^[27], coprecipitation^[28], combustion^[29], and conventional solid-state reaction^[30]. Due to the fascinating luminescence properties of CaMoO₄, in the current study, a ultrasonic method was applied to synthesize CaMoO₄ nanoparticles to investigate its photocatalytic properties. In order to enhance the photocatalytic properties of the as-synthesized CaMoO₄ nanoparticles, graphene oxide was used to make a hybrid nanocomposite (CaMoO₄@GO). Besides, methylene blue (MB) was used to measure the photocatalytic ability of CaMoO₄ nanoparticles and its nanocomposite (CaMoO₄@GO) under Uv-Vis light.

2. Characterization

X-ray diffraction (XRD) patterns were recorded by a Philips-X'PertPro, X-ray diffractometer using Ni-filtered Cu K α radiation at the scan range of $10 < 2\theta < 80$. Scanning electron microscopy (SEM) images were obtained on LEO-1455VP equipped with an energy dispersive X-ray spectroscopy. The energy dispersive spectrometry (EDS) analysis was studied by XL30, Philips microscope. Ultrasonic irradiation was performed using a high-intensity ultrasonic probe (Sonicator 3000; Bandeline, MS 72, Germany, Tihorn, 20kHz, 60Wcm⁻²) immersed directly in the reaction solution.

3. Synthesis of CaMoO₄ nanoparticles

All the chemicals used were of analytical grade and without any further purification. The stoichiometric ratio of (NH₄)₆Mo₇O₂₄·4H₂O and Ca(NO₃)₂·6H₂O were dissolved in 30ml of distilled water, separately. Then, after heating Ca(NO₃)₂·6H₂O solution up to 50°C for 10min, (NH₄)₆Mo₇O₂₄·4H₂O solution was added dropwise to it. Eventually, the final mixed solution was ultrasonicated at 100W for 30min. After ultrasonication, the mixture was cooled to room temperature naturally and the obtained white precipitate was collected by filtration, washed with absolute ethanol and distilled water several times, and was dried in vacuum at 50°C for 120 min.

4. Synthesis of CaMoO₄@GO nanocomposites

In order to synthesize semiconductor nanocomposite (CaMoO₄@GO), various molar ratios of graphene oxide were mixed with CaMoO₄ nanoparticles under ultrasonic waves (100W) for 20min. After irradiation, the precipitates were washed, centrifuged, and dried in vacuum at 60°C for 2h.

5. Photocatalytic experiments

Photodegradation of Methylene blue (MB) under Uv-Vis light was performed in the presence of CaMoO₄ nanoparticles and its nanocomposite (CaMoO₄@GO) to investigate their photocatalytic properties and subsequently the impact of GO on the photocatalytic properties of CaMoO₄ nanoparticles. Photodegradation experiments were run in the presence of CaMoO₄/CaMoO₄@GO (20mg) and MB solution (150mL of 5mg/L solution) under Uv-Vis light. Before exposing to the light, the mixture solution of dye and nanoparticles was kept in darkness (30min) in order to establish adsorption-desorption equilibrium between the dye molecules and nanoparticle surface. After 30min, it was exposed to the 500W Xe lamp while 10mL of mixture solution was taken out (each 15min), centrifuged, and their absorbances were recorded. The MB degradation percentage was calculated as:

$$\text{Degradation rate (\%)} = 100 (A_0 - A)/A_0$$

where A₀ and A are the absorbance value of the solution at A₀ and A min, respectively.

6. Results and discussion

Figure 1. a-c shows the XRD patterns of CaMoO₄ nanoparticles, GO, and CaMoO₄@GO nanocomposites, respectively. Figure 1. a indicates the formation of tetragonal phase of CaMoO₄ with calculated cell parameters a = b = 5.2260 Å and c = 11.4300Å, space group of I41/a, and JCPDS No. 29-0351. Based on the XRD pattern of GO (Figure 1. b), the peak at 2θ = 12.5° is assigned to the GO (002)^[31]. Moreover, the XRD spectrum of CaMoO₄@GO nanocomposites (Fig. 1c) demonstrates tetragonal phase of CaMoO₄ (space group I41/a and JCPDS No.29-0351) along with the peak at 2θ = 12.5°, related to the GO. Based on the Debye Scherrer Eq. (1) and XRD data, the crystallite diameter (D_c) of CaMoO₄ nanoparticles and CaMoO₄@GO nanocomposites are measured to be 23nm and 19.5nm, respectively:

$$D_c = K\lambda/\beta\cos\theta \quad (1)$$

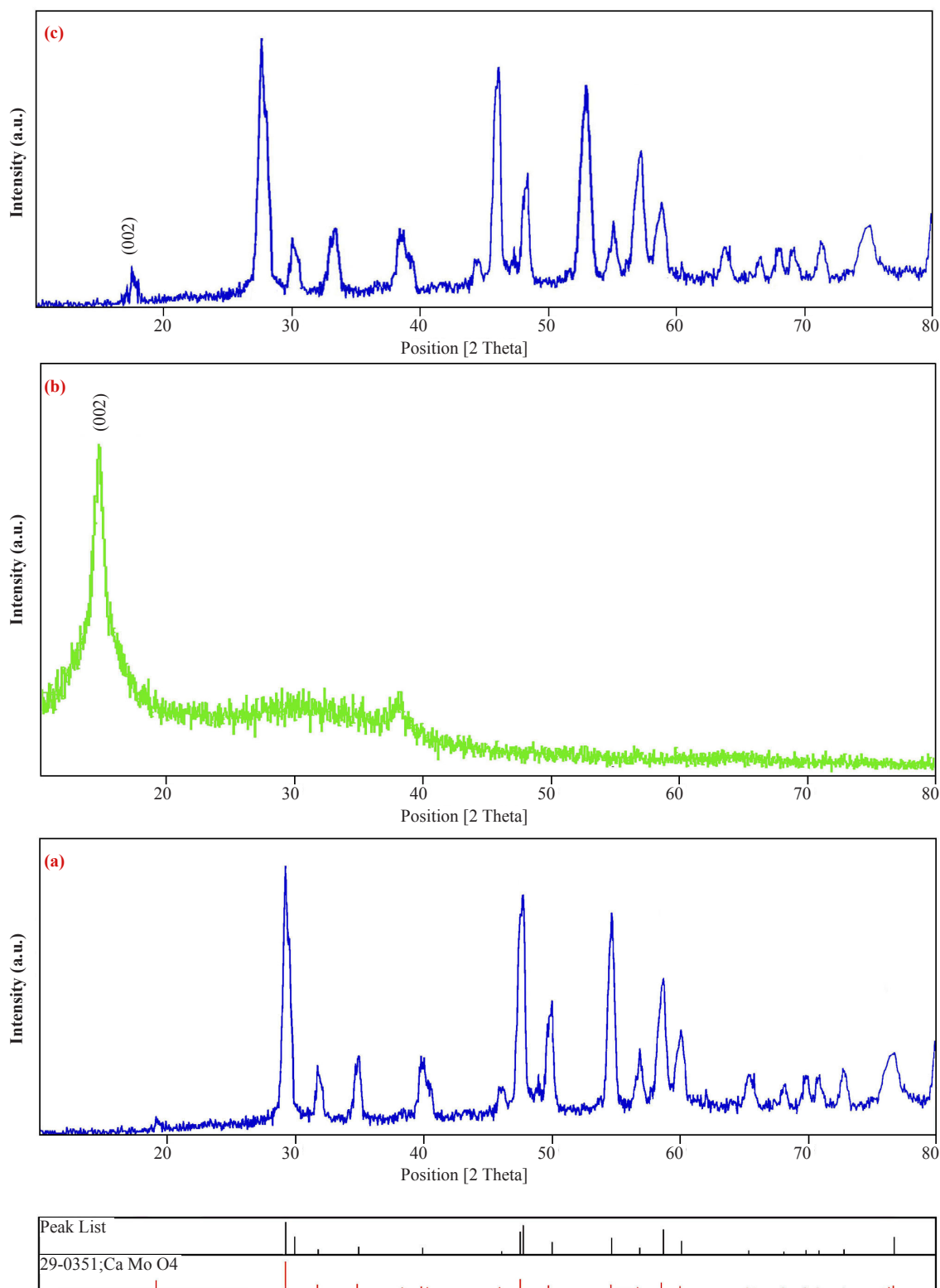


Figure 1. XRD patterns of (a) CaMoO_4 nanoparticles (b) GO (c) CaMoO_4 @GO nanocomposites

where β is the breadth of the observed diffraction line at its half intensity maximum, K is the so-called shape factor, which usually takes a value of about 0.9, and λ is the wavelength of X-ray source used in XRD. Doping the GO into the CaMoO_4 nanoparticles causes the crystal size to decrease from 23nm to 19.5nm. In other words, XRD characteristic peaks of CaMoO_4 in nanocomposite are broader than those in pure CaMoO_4 nanoparticles which could be related to the increasing the nucleation sites due to the increase in the functional groups as a result of doping GO^[32-33]. Energy-

dispersive X-ray spectroscopy (EDS) was applied to further examine the purity of CaMoO_4 nanoparticles, as shown in Figure 2. EDS analysis shows that CaMoO_4 consists of only Ca, Mo, and O elements. Scanning electron microscopy was used to investigate the morphology of GO, CaMoO_4 nanoparticles, and CaMoO_4 @GO nanocomposites, as shown in Figure 3. a-c, respectively. SEM images of CaMoO_4 nanoparticle and GO show that they mainly consists of spherical nanoparticles and sheet structure, respectively. In addition, CaMoO_4 @GO nanocomposites SEM images show that CaMoO_4 @GO composed of sheets and nanoparticles. Tauc's relationship ($\alpha = \alpha_0(h\nu - E_g)^n/h\nu$) has been using to measure the electronic bandgap of semiconductors. Where α ($\alpha = 2.303A/t$) is the absorption coefficient, h and ν are Planck's constant and the photon energy, respectively. In addition, α_0 is the constants, E_g is the optical band gap of the material, and n depends on the type of electronic transition and can be any value between $\frac{1}{2}$ and 3. The band gaps of CaMoO_4 , GO, and CaMoO_4 @GO nanocomposites, with various GO concentrations, could be calculated through the extrapolating the linear portion of the plots of $(\alpha h\nu)^{1/2}$ against $h\nu$ to the energy axis, as shown in Figure 4. The bandgaps of CaMoO_4 and CaMoO_4 @GO nanocomposites (GO = 0.02 to 0.1g corresponding to the samples 1-5) are 3.3, 3.29, 3.15, 3.14, 3.1, and 3eV, respectively. Doping the GO into the CaMoO_4 nanoparticles, narrows its bandgap energy and shift absorption edge towards higher wavelengths due to an increase of surface charge in presence of GO which is thanks to the unpaired π electrons of GO surface. As a result, absorption ability of CaMoO_4 @GO nanocomposites was enhanced in the visible light region. Methylene blue (MB), an organic pollutant, was selected in order to assess the photocatalytic properties of CaMoO_4 and CaMoO_4 @GO nanocomposites under Uv-Vis light, as shown in Figure 5. Based on Figure 5, in the presence of CaMoO_4 nanoparticles, MB was degraded 65%. On the other hand, doping GO into the CaMoO_4 nanoparticles causes increase degradation by 89% after 90min (Table 1). The enhancing photodegradation mechanism of MB in the presence of CaMoO_4 @GO nanocomposites can be explain as follows^[34-35]. At first, light induces MB dye molecules to the higher energy level in which a photoexcited e^- from VB of CaMoO_4 jumps to its CB follow by jumping into the GO. GO, as an electron acceptor, acts as a suppressive agent which suppresses the recombination of charge carriers due to its two-dimensional π -conjugation structure. Afterwards, electrons from GO react with environmental oxygen to create superoxide radicals ($\text{O}_2^{\cdot -}$) and then holes in the VB react with H_2O_2 to create hydroxyl radicals (OH°). Finally, intermediates, water, and CO_2 produce due to the oxidizing MB by OH° and $\text{O}_2^{\cdot -}$ species. By comparing to other published works, the current study shows maximum photocatalyst yield in lower degradation time, due to the presence of GO^[36-37].

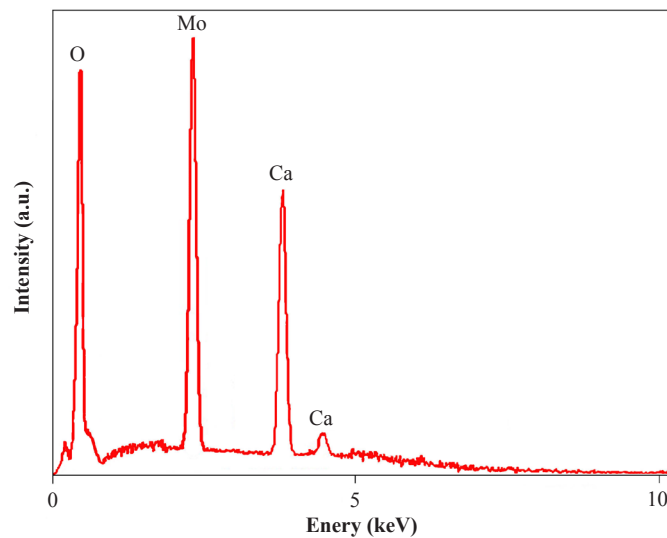


Figure 2. EDS pattern of CaMoO_4 nanoparticles

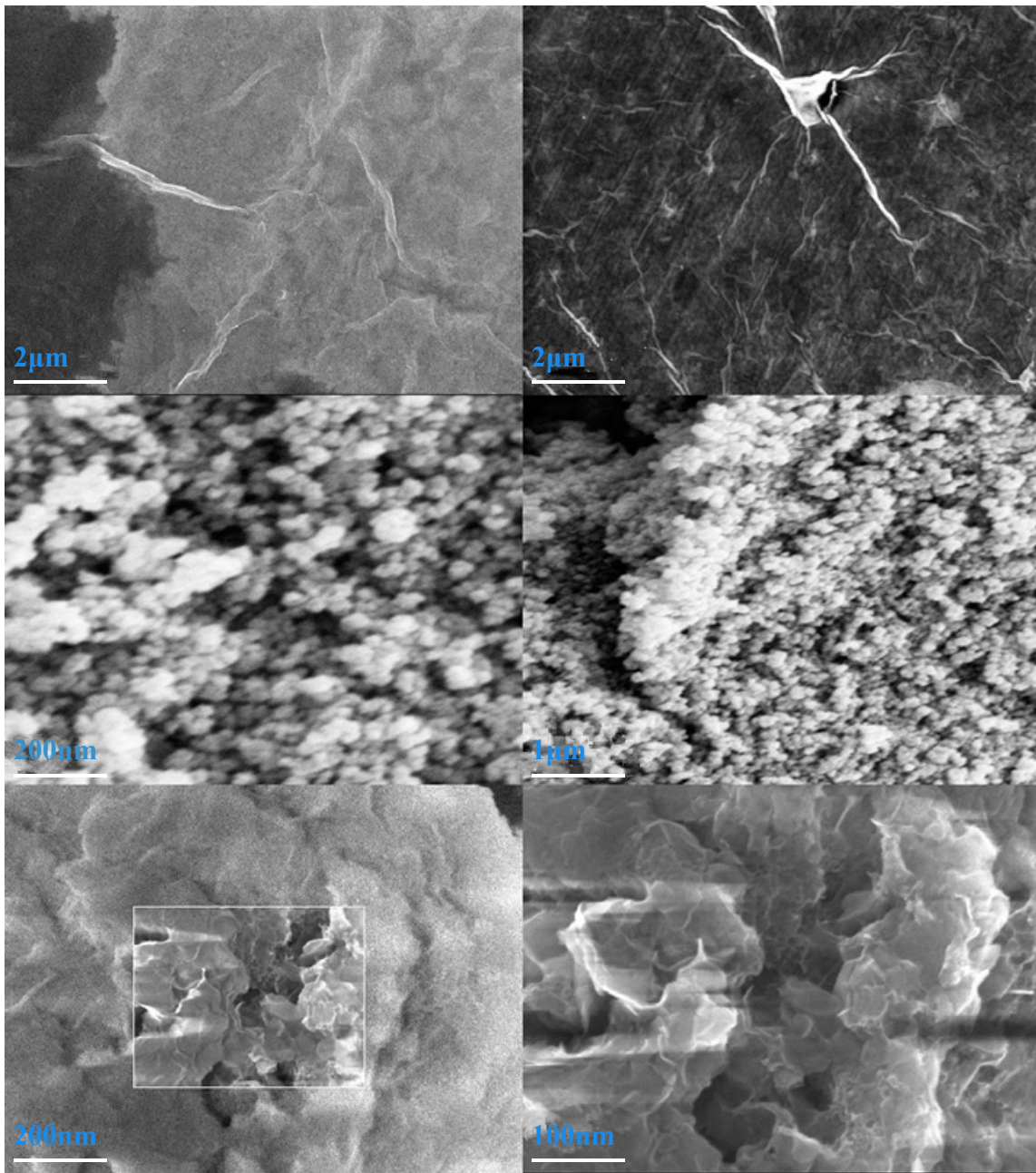


Figure 3. SEM images of (a) GO (b) CaMoO_4 nanoparticles (c) CaMoO_4 @GO nanocomposites

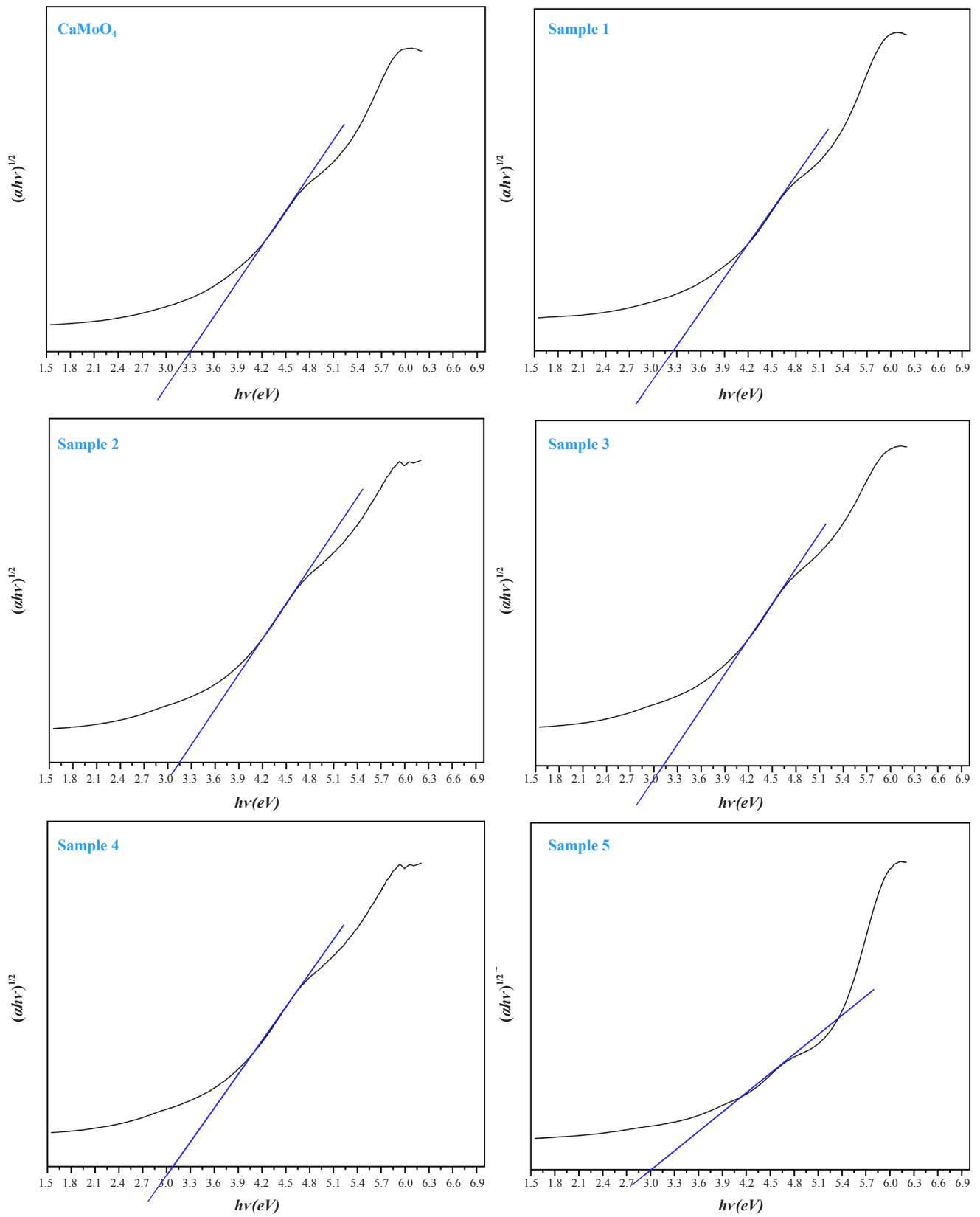


Figure 4. UV-Vis patterns of CaMoO₄ and CaMoO₄@GO nanocomposites

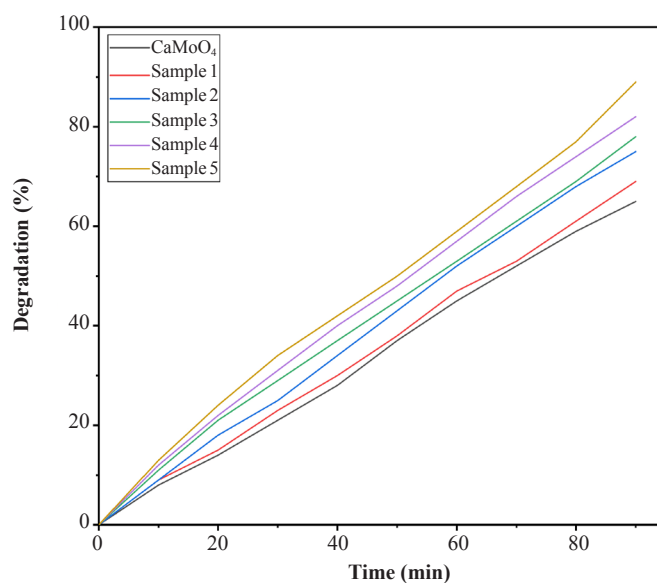


Figure 5. Photodegradation of MB in the presence of CaMoO₄ nanoparticles and CaMoO₄@GO nanocomposites (sample 1-5)

Table 1. Degradation yield of MB in the presence of CaMoO₄ nanoparticles and CaMoO₄@GO nanocomposites (sample 1-5)

Sample No	MB Degradation (%)	Band Gap (eV)
CaMoO ₄	65	3.3
1	69	3.29
2	75	3.15
3	78	3.14
4	82	3.1
5	89	3

7. Conclusions

In summary, CaMoO₄ and its composite (CaMoO₄@GO) were synthesized under the ultrasonic wave. The impacts of various graphene oxide concentrations on the optical and photocatalytic properties of CaMoO₄ were investigated. Degradation of methylene blue (MB) was examined to evaluate the photocatalytic properties of CaMoO₄ and CaMoO₄@GO. Photodegradation results revealed that increasing the GO concentration causes to increase in the degradation percentage of MB due to the increase visible light absorption by CaMoO₄@GO nanocomposites.

8. Acknowledgment

The authors are grateful to the council of the University of Arak for providing financial support to undertake this work and Padideh Noavaran Nano Bonyan Company, Iran.

References

- [1] Evgenidou E, Konstantinou I, Fytianos K, et al. Photocatalytic oxidation of methyl parathion over TiO₂ and ZnO suspensions. *Catal. Today*. 2007; 124: 156-162.
- [2] Tu S, Zhang Y, Reshak A. H, et al. Ferroelectric polarization promoted bulk charge separation for highly efficient CO₂ photoreduction of SrBi₄Ti₁₄O₁₅. *Nano Energy*. 2019; 56: 840-850.
- [3] Reshak A. H. Active photocatalytic water splitting solar-to-hydrogen energy conversion: Chalcogenide photocatalyst Ba₂ZnSe₃ under visible irradiation. *Applied Catalysis B: Environmental*. 2018; 221: 17-26.
- [4] Reshak A. H. Sulfide oxide XZnSO (X = Ca or Sr) as novel active photocatalytic water splitting solar-to-hydrogen energy conversion. *Applied Catalysis B: Environmental*. 2018; 225: 273-283.
- [5] Reshak A. H. A novel photocatalytic water splitting solar-to-hydrogen energy conversion: Non-centro-symmetric borate CsZn₂B₃O₇ photocatalyst. *J. Alloys Compd*. 2018; 741: 1258-1268.
- [6] Huang H, Reshak A. H, Auluck S, et al. Visible-light-responsive sillén-structured mixed-cationic CdBiO₂Br

- nanosheets: layer structure design promoting charge separation and oxygen activation reactions. *Phys. Chem. C*. 2018; 122(5): 2661-2672.
- [7] Reshak A. H. Novel photocatalytic water splitting solar-to-hydrogen energy conversion: CdLa₂S₄ and CdLa₂Se₄ ternary semiconductor compounds. *Chem. Chem. Phys.* 2018; 20: 8848-8858.
- [8] Reshak A. H. Chairlike and boatlike graphane: Active photocatalytic water splitting solar-to-hydrogen energy conversion under UV irradiation. *Phys. Chem. C*. 2018; 122: 8076-8081.
- [9] Reshak A. H. AA- and ABA-stacked carbon nitride (C₃N₄): novel photocatalytic water splitting solar-to-hydrogen energy conversion. *Phys. Chem. Chem. Phys.* 2018; 20: 22972-22979.
- [10] Hosseinpour-Mashkani S. M, Maddahfar M, Sadeghinia A, et al. PbSe@PbSO₄ nanoparticles: sonochemical synthesis and characterization and its photocatalytic degradation of methylene blue. *Journal of Materials Science: Materials in Electronics*. 2015; 26: 3352-3356.
- [11] Gholami A, Nikkhah-Amirabad T, Maddahfar M. Investigation of photovoltaic properties of silver-doped ZnTiO₃ nanoparticles. *Journal of Materials Science: Materials in Electronics*. 2017; 28: 15327-15332.
- [12] Gholami A, Maddahfar M. Synthesis and characterization of barium molybdate nanostructures with the aid of amino acids and investigation of its photocatalytic degradation of methyl orange. *Journal of Materials Science: Materials in Electronics*. 2016; 27: 6773-6778.
- [13] Hosseinpour-Mashkani S. M, Maddahfar M, Sobhani-Nasab A. Precipitation synthesis, characterization, morphological control, and photocatalyst application of ZnWO₄ nanoparticles. *Journal of Electronic Materials*. 2016; 45: 3612-3620.
- [14] Gholami A, Maddahfar M. Synthesis and characterization of novel samarium-doped CuAl₂O₄ and its photocatalytic performance through the modified sol-gel method. *Journal of Materials Science: Materials in Electronics*. 2016; 27: 3341-3346.
- [15] Hosseinpour-Mashkani S. M, Maddahfar M, Sobhani-Nasab A. Novel silver-doped CdMoO₄: synthesis, characterization, and its photocatalytic performance for methyl orange degradation through the sonochemical method. *Journal of Materials Science: Materials in Electronics*. 2016; 27: 474-480.
- [16] Maddahfar M, Ramezani M, Sadeghi M, et al. NiAl₂O₄ nanoparticles: synthesis and characterization through modify sol-gel method and its photocatalyst application. *Journal of Materials Science: Materials in Electronics*. 2015; 26: 7745-7750.
- [17] Cornu L, Jubera V, Demourgues A, et al. Luminescence properties and pigment properties of A-doped (Zn, Mg) MoO₄ triclinic oxides (with A = Co, Ni, Cu or Mn). *Ceramics International*. 2017; 43: 13377-13387.
- [18] Cho W. S, Yashima M, Kakihana M, et al. Active electrochemical dissolution of molybdenum and application for room-temperature synthesis of crystallized luminescent calcium molybdate film. *J. Am. Ceram. Soc.* 1997; 8: 765-769.
- [19] Musikhin A. E, Naumov V. N, Bespyatov M. A, et al. Heat capacity and thermodynamic functions of CaMoO₄ at low temperatures. *J. Alloys Compd.* 2016; 655: 165-171.
- [20] Sarantopoulou E, Raptis C, Ves S, et al. Temperature and pressure dependence of Raman-active phonons of CaMoO₄: an anharmonicity study. *J. Phys. Condens. Matter*. 2002; 14: 8925-8938.
- [21] Han Y, Wang L, Wang D, et al. Lanthanide ions-doped calcium molybdate pie-like microstructures: Synthesis, structure characterization, and luminescent properties. *J. Alloys Compd.* 2017; 695: 3018-3023.
- [22] Laguna M, Nuñez N. O, Becerro A. I, et al. Morphology control of uniform CaMoO₄ microarchitectures and development of white light emitting phosphors by Ln doping (Ln = Dy³⁺, Eu³⁺). *Cryst Eng Comm.* 2017; 19: 1590-1600.
- [23] Ponta O, Ciceo Lucacel R, Vulpoi A, et al. Synthesis and characterisation of nanostructured silica-powellite-HAP composites. *J. Mater. Sci.* 2015; 50: 577-586.
- [24] Li X, Fan G, Huang Z. Synthesis and surface thermodynamic functions of CaMoO₄ nanocakes. *Entropy*. 2015; 17: 2741-2748.
- [25] Bhanvase B. A, Kadam V. B, Rode T. D, et al. Sonochemical process for the preparation of novel calcium zinc molybdate nanoparticles. *Int. J. Nanosci.* 2015; 14: 1550014-1550023.
- [26] Kusuma M, Chandrappa G. T. Effect of calcination temperature on characteristic properties of CaMoO₄ nanoparticles. *Journal of Science: Advanced Materials and Devices*. 2019; 4: 150-157.
- [27] Grasser R, Pitt E, Scharmann A, et al. Optical properties of CaWO₄ and CaMoO₄ crystals in the 4 to 25eV region. *Phys. Status Solidi B*. 1975; 69: 359-368.
- [28] Paski E. F, Blades M. W. Analysis of inorganic powders by time wavelength resolved luminescence spectroscopy. *Anal. Chem.* 1988; 60: 1224-1230.
- [29] Yang P, Yao G. Q, Lin J. H. Photoluminescence and combustion synthesis of CaMoO₄ doped with Pb²⁺. *Inorg. Chem. Commun.* 2004; 7: 389-391.

- [30] Sleight A. W. Accurate cell dimensions for ABO_4 molybdates and tungstates. *Acta Crystallogr. B: Struct. Crystallogr. Cryst. Chem.* 1972; 28: 2899-2902.
- [31] Shalaby A, Nihtianova D, Markov P, et al. Structural analysis of reduced graphene oxide by transmission electron microscopy. *Bulgarian Chemical Communications.* 2015; 47: 291-295.
- [32] Dreyer D. R, Park S, Bielawski C. W, et al. The chemistry of graphene oxide. *Chem. Soc. Rev.* 2010; 39: 228-240.
- [33] Abrinaeia F, Kimiagarb S, Zolghadrc S. Hydrothermal synthesis of hematite-GO nanocomposites at different GO contents and potential application in nonlinear optics. *Optical Materials.* 2019; 96: 109285.
- [34] Giovannetti R, Rommozzi E, Zannotti X, et al. Recent advances in graphene based TiO_2 nanocomposites ($GTiO_2N_s$) for photocatalytic degradation of synthetic dyes. *Catalysts.* 2017; 7: 305-339.
- [35] Li B, Liu T, Wang Y, et al. ZnO/graphene-oxide nanocomposite with remarkably enhanced visible-light-driven photocatalytic performance. *J. Colloid Interface Sci.* 2012; 377: 114-121.
- [36] Huerta-Flores A. M, Juárez-Ramírez I, Torres-Martínez L. M, et al. Synthesis of $AMoO_4$ (A = Ca, Sr, Ba) photocatalysts and their potential application for hydrogen evolution and the degradation of tetracycline in water. *Journal of Photochemistry and Photobiology A: Chemistry.* 2018; 356: 29-37.
- [37] Hosseinpour-Mashkani S. S, Hosseinpour-Mashkani S. S, Sobhani-Nasab A. Synthesis and characterization of rod-like $CaMoO_4$ nanostructure via free surfactant sonochemical route and its photocatalytic application. *J. Mater. Sci. Mater. Electron.* 2016; 27: 4351-4355.